Shear-wave studies of the near-surface at the CaMI Field Research Station in Newell County, Alberta

Don C. Lawton, J. Helen Isaac and Malcolm Bertram

ABSTRACT

Two S-wave seismic surveys were acquired at the CaMI Field Research Station (FRS) in the summer of 2018 using Echo Seismic Ltd's S-wave Envirovibe. For the first survey receivers were placed every 10 m in a fixed array and the source interval was 20 m. The second survey consisted of a 72-m streamer array towed behind the truck. The source interval was 2 m and the receiver interval was 1 m. The recorded S-wave data are of good quality with clear first breaks. A smoothed S-wave velocity model was derived from refraction statics analysis. The near-surface S-wave low velocity layer is 28.5 to 34.5 m thick, with velocities ranging from 222 to 280 m/s. The S-wave bedrock velocity ranges between 1045 and 1110 m/s. The depths to bedrock compare well with the actual bedrock depth of 29.5 m at the injection well location. We applied some basic processing to both surveys, stacked and migrated them. The streamer array line images the bedrock very well. This line was converted to depth using the refraction velocities. The depth of imaged bedrock compares very well with the true bedrock depth of 29.5 m at the injection well.

Application of the receiver statics derived from the fixed array survey to the PS data acquired in 2017 improved the imaging of the Basal Belly River reflector on stacked sections.

INTRODUCTION

The Containment and Monitoring Institute (CaMI), established by CMC Research Institutes Inc, has a Field Research Station (FRS) near Brooks, Alberta, where technologies for the measurement, monitoring and containment of subsurface fluids, including carbon dioxide, are being developed, refined and calibrated. A well for injection of CO_2 was drilled in 2015 to a depth of 550 m and small amounts (up to 400 tonnes per year) of CO_2 are being injected into the Upper Cretaceous Basal Belly River Formation, which is a water-wet sandstone capped by the shales, silts and silty sands of the Belly River Formation.

S-WAVE SEISMIC DATA

Two S-wave seismic surveys were acquired at the FRS in the summer of 2018. The locations of the lines were very close to line 13 from previous P-wave surveys and were both around 1.1 km long, running SW-NE past the injection well. For the first survey the source was Echo Seismic Ltd.'s S-wave Envirovibe, which has a base plate that imparts an S-wave source. The source was about 5 m offset from the fixed array of 111 3C geophones. Shots were acquired every 20 m using a source sweep of 10-150 Hz. The field data show frequency content diminishing after 50 Hz.

The second survey was acquired by Echo Seismic Ltd and consisted of a streamer array towed behind their S-wave Envirovibe. The source interval was 2 m and the receiver interval was 1 m. The streamer was 72 m long. Figure 1 is a picture of the multicomponent land streamer and Figure 2 shows the S-wave Envirovibe source.

FIG 1. Echo Seismic Ltd. multicomponent land streamer.

The recorded reflected S-wave data are of good quality with clear first breaks. The fixed array data (Figure 3a) indicate a near-surface S-wave velocity around 250 m/s and a refractor with a velocity of 1140 m/s intercepting at an offset of 60 m on Figure 1a. We did not see refracted arrivals on the streamer data as the offsets were too short. However, the first break times implied near-surface velocities similar to those seen on the fixed array data. We picked the first breaks and did refraction statics analysis. The results of this analysis gave a near-surface S-wave velocity/depth model and a set of shear shot and receiver statics. Figure 4 shows the smoothed S-wave velocity model. The near-surface S-wave low velocity layer is 28.5 to 34.5 m thick, with velocities ranging from 222 to 280 m/s. The S-wave bedrock velocity ranges between 1045 and 1110 m/s. The results of this analysis compare well with the actual bedrock depth of 29.5 m at the injection well location.

FIG 2. Echo Seismic Ltd.'s S-wave Envirovibe and land streamer.

We used these refraction velocities as a guide function for semblance velocity analysis and picked rms velocities on the fixed array data. The few stacking velocities we were able to pick were a little higher than the refraction velocities but resulted in a better looking stacked section than obtained using the refraction velocity model.

We applied some basic processing, including noise attenuation and Gabor deconvolution (Margrave and Lamoureux, 2002), to both surveys, stacked and migrated them. The results are shown in Figure 5. The fixed array line has some noise and does not reveal any significant reflectors. The streamer array line, on the other hand, images the bedrock very well at around 0.3 s. This line was converted to depth (Figure 6) using the refraction velocities. The depth of imaged bedrock compares very well with the true bedrock depth of 29.5 m at the injection well.

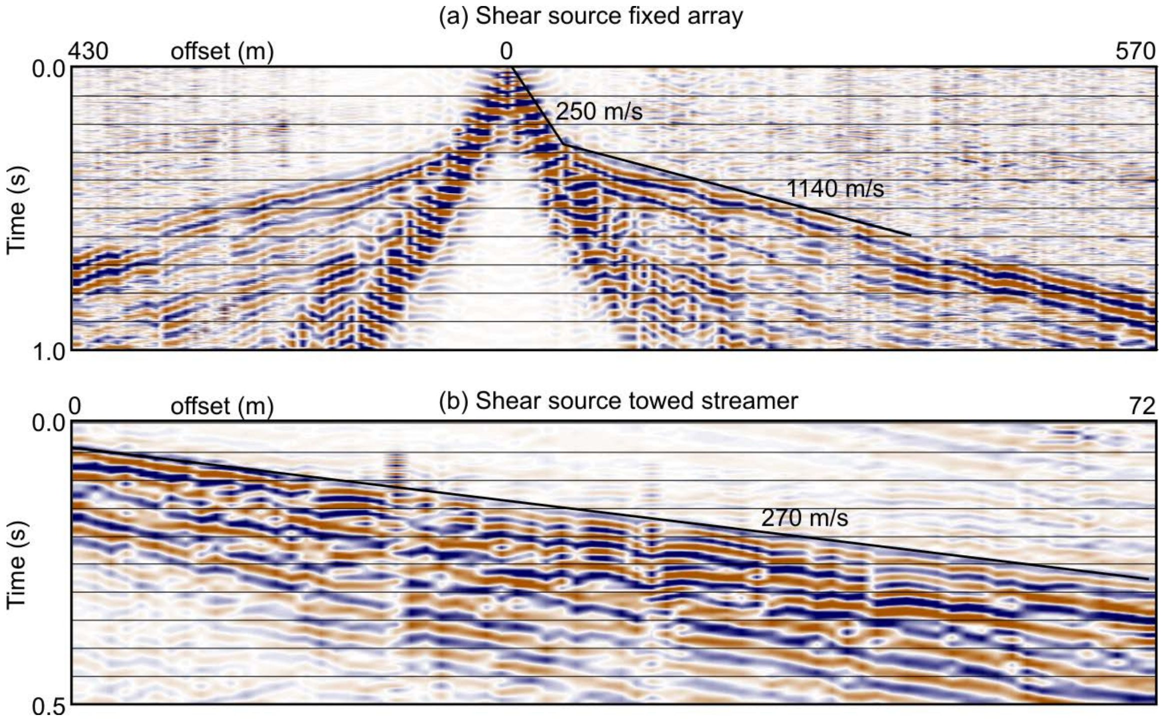

FIG. 3. Shot gathers from the (a) fixed receiver and (b) towed streamer S-wave surveys. First breaks on these particular gathers indicate near-surface velocities of 250-270 m/s and a bedrock velocity of 1140 m/s.

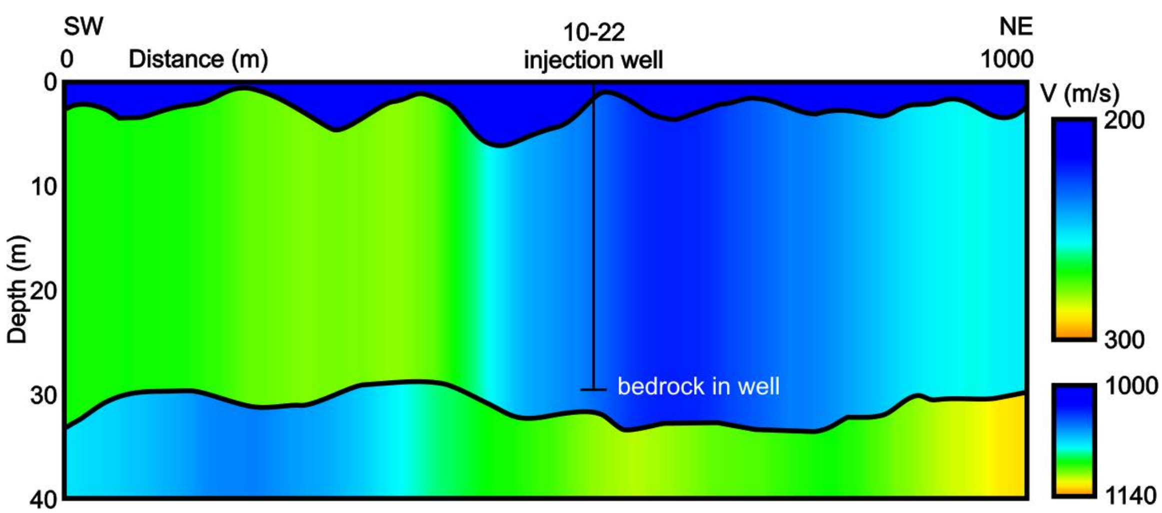

FIG. 4. The depth/velocity model derived from refraction analysis. Near-surface velocities are 222-280- m/s and bedrock velocities are 1040-1110 m/s. Bedrock depth varies from 28.5-34.5 m. The actual depth of bedrock at the well location is 29.5 m.

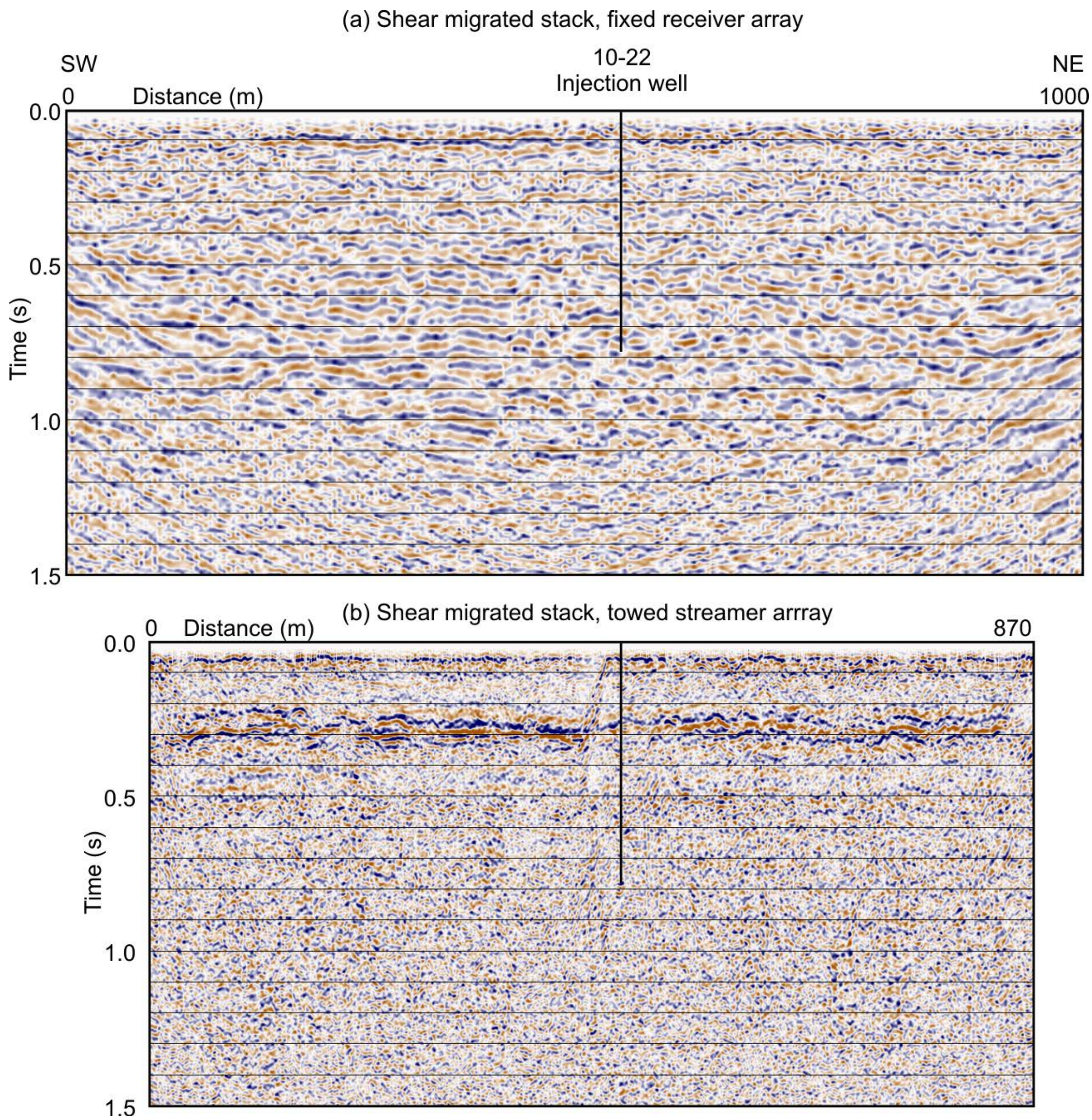

FIG. 5. Migrated (a) fixed array data and (b) streamer array data.

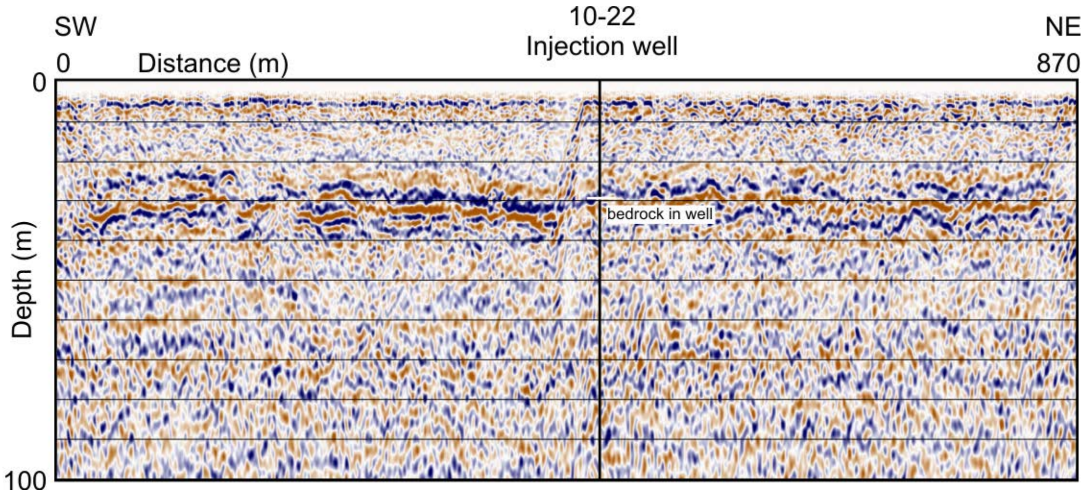

FIG. 6. Migrated streamer array section converted to depth using the velocity model in Figure 1 averaged to a single function. The imaged depth of bedrock compares well to the bedrock depth in the injection well.

Receiver Statics

We smoothed the receiver statics obtained from the fixed array survey and applied them to the PS survey acquired in 2017. We had estimated receiver statics for that data by flattening a receiver stack and we wanted to compare these results with those obtained using the 2018 S-wave receiver statics. Figure 7 shows two receiver stacks; one with no receiver refraction statics (a) and one with the smoothed receiver refraction statics from the S-wave survey (b). Elevation statics to final datum have been applied in both cases. Receiver stacks of data acquired in areas with a large variation in the S-wave near-surface velocities will show great variability in reflection times across the section. Receiver stack 7a, which has no receiver statics, shows that receiver statics are not a problem in this area. A simple common approach to estimating receiver statics is to flatten a reflector on a receiver gather and use those flattening time shifts as the receiver statics. Both stacks were flattened to observe the effect of applying additional receiver statics, resulting in the stacks in Figure 8. These stacks show that it is not possible to flatten all the reflectors based upon flattening a single reflector so the technique is not entirely satisfactory.

We also created common conversion point (CCP) stacks with no receiver statics and with the shear receiver statics (Figure 9). The CCP stack with statics (9b) has better continuity in the centre of the line, especially on the target Basal Belly River event at about 0.5 s, but the deepest event at 1.5 s is not flattened as well as in Figure 7a. The CCP stacks after application of the additional receiver statics are shown in Figure 10. Figure 10b, based upon the 2018 S-wave statics, shows greater continuity of the reflector at 0.6 s so we infer that inclusion of the S-wave statics has helped to improve the imaging.

The total receiver statics applied to the stacks in Figure 10 are graphed in Figure 11. They show a very similar distribution of values.

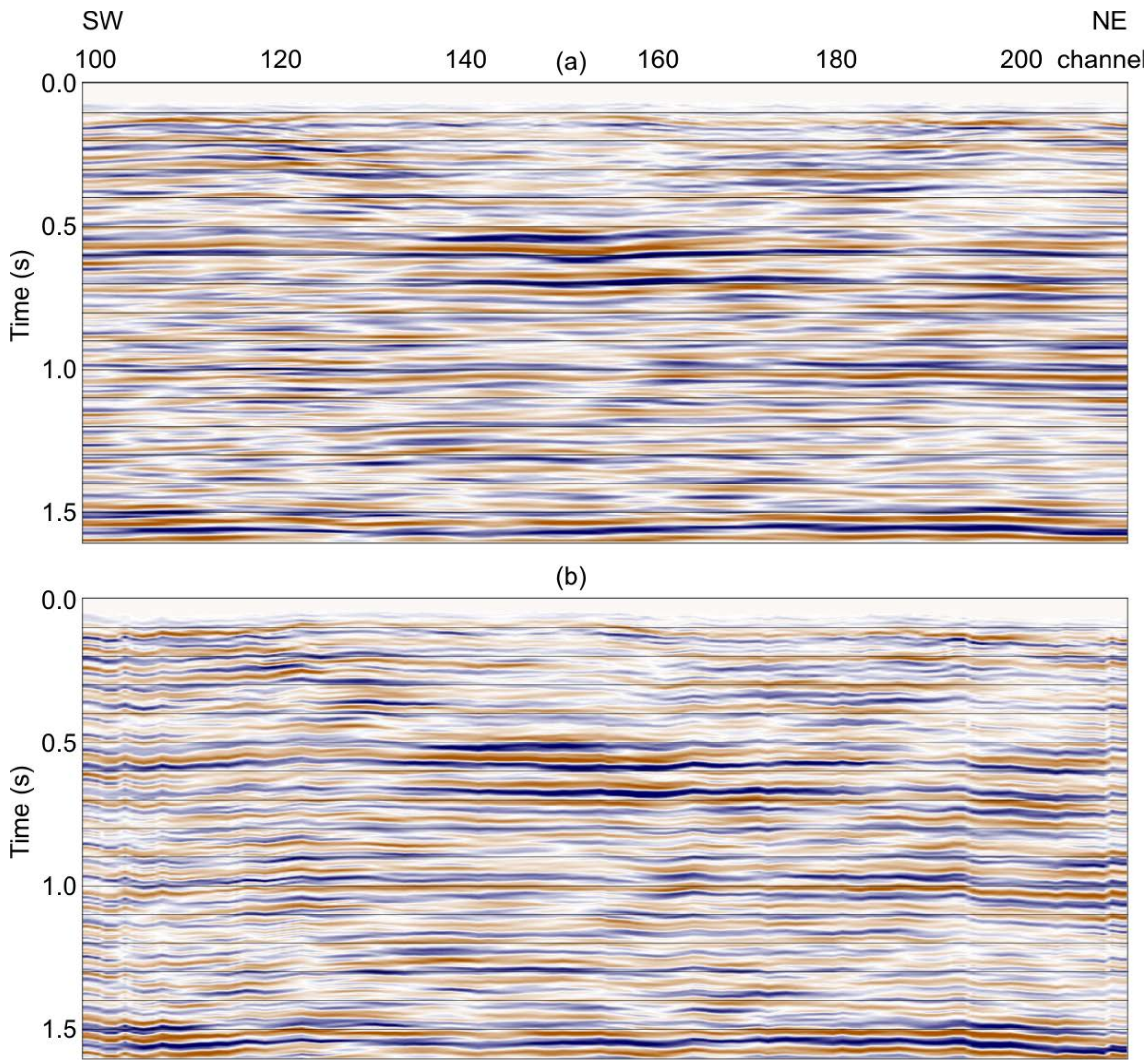

FIG. 7. Receiver stacks of the 2017 PS data with elevation statics to final datum and (a) no additional statics, and (b) receiver statics from the 2018 fixed array S-wave survey. The Basal Belly River reflection is the strong event near 0.5 s.

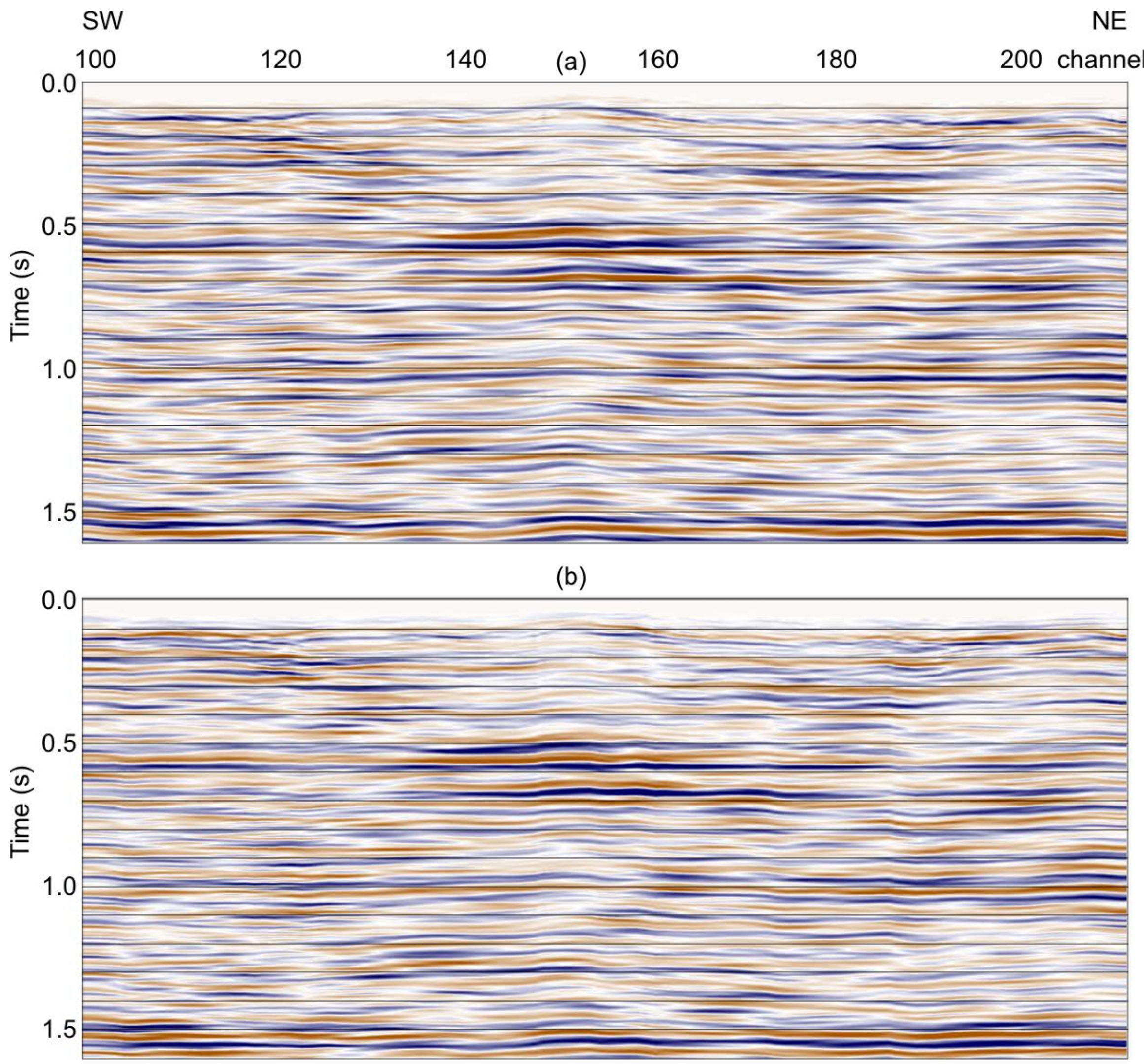

FIG. 8. Flattened versions of the 2017 PS receiver stacks in Figure 5.

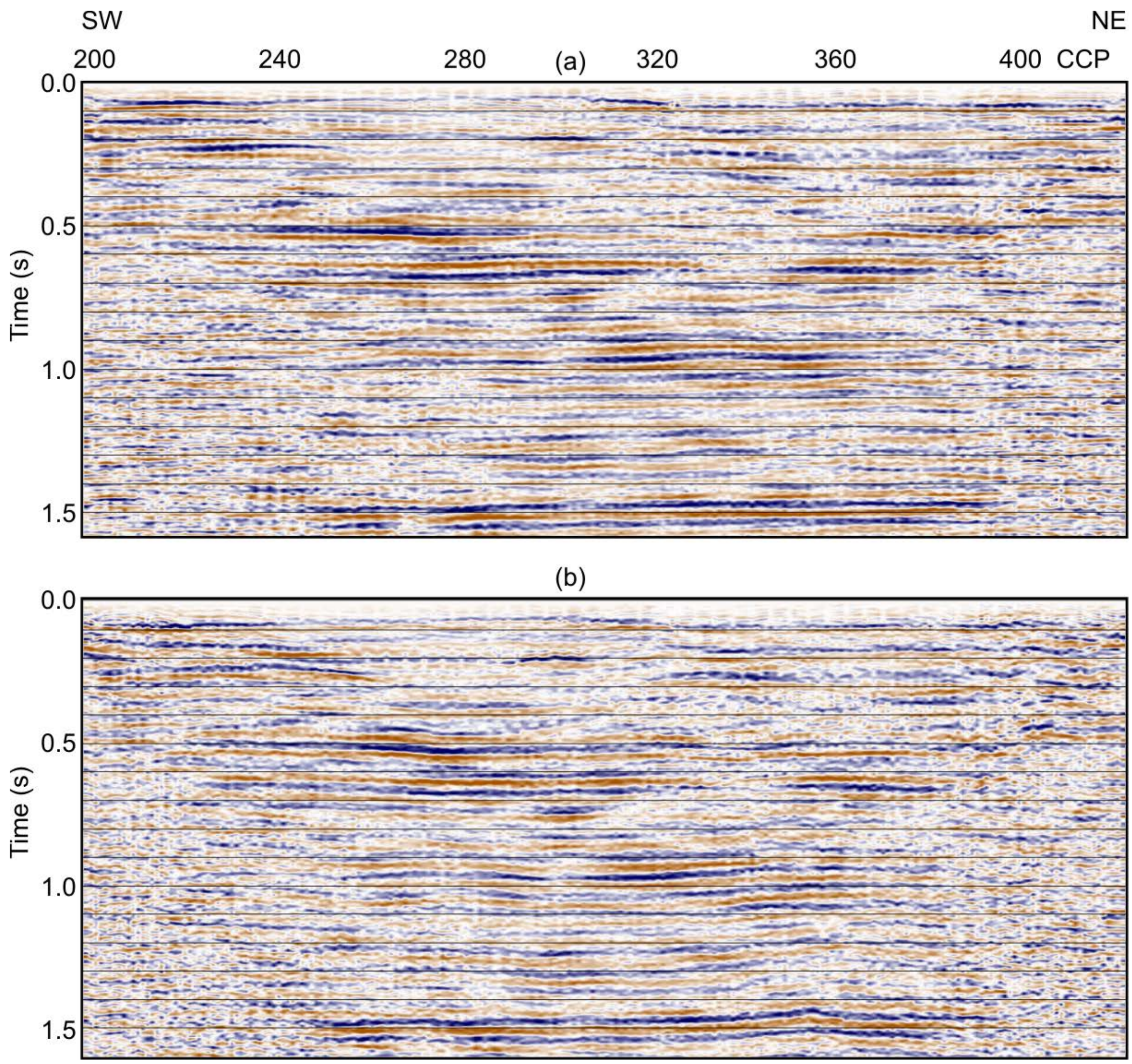

FIG. 9. Common conversion point (CCP) stacks of the 2017 PS data with (a) no additional statics, and (b) receiver statics from the 2018 fixed array S-wave survey.

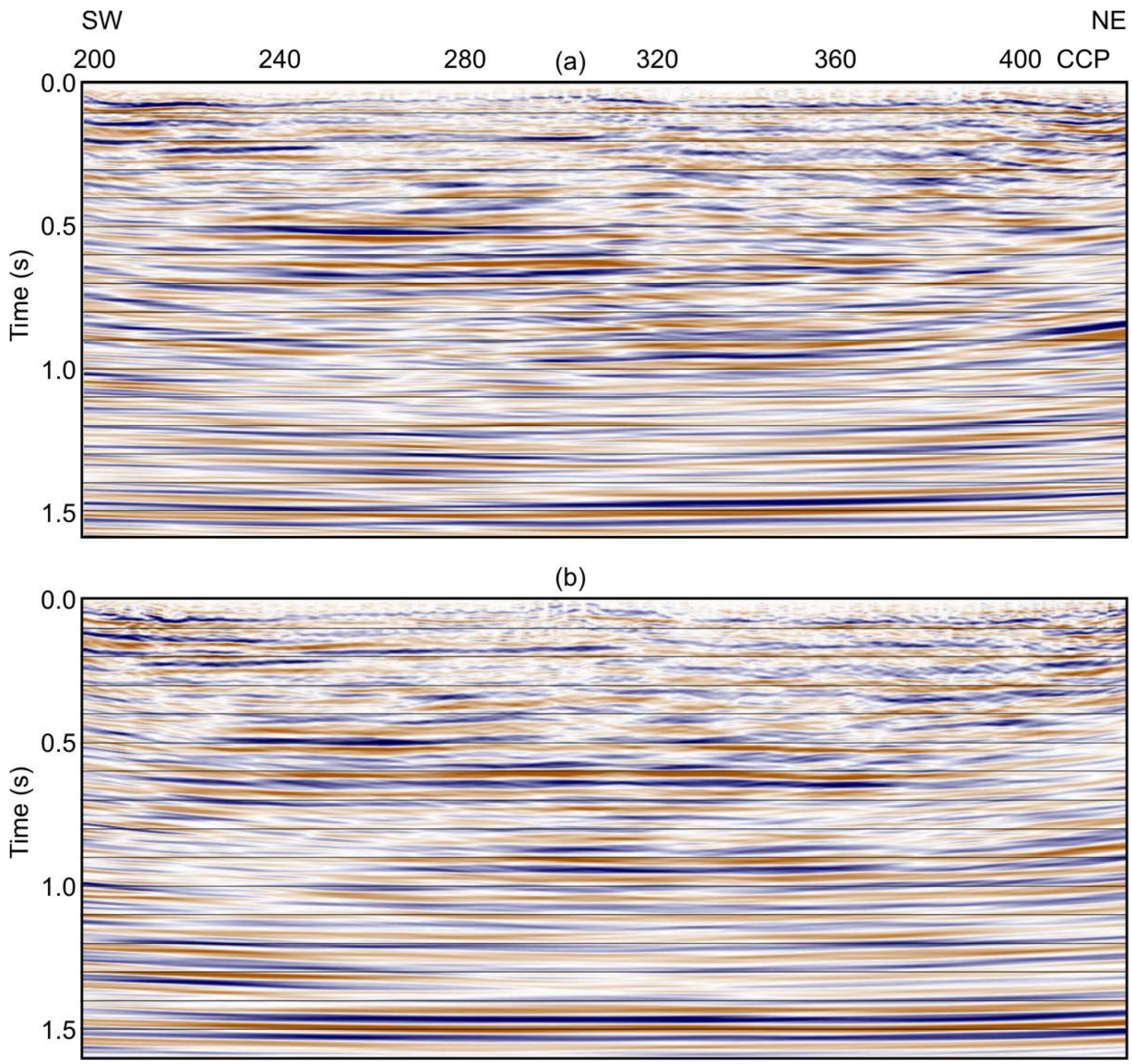

FIG. 10. Migrated CCP stacks of the 2017 PS data with (a) flattening receiver statics, and (b) receiver statics from the 2018 fixed array S-wave survey and flattening receiver statics.

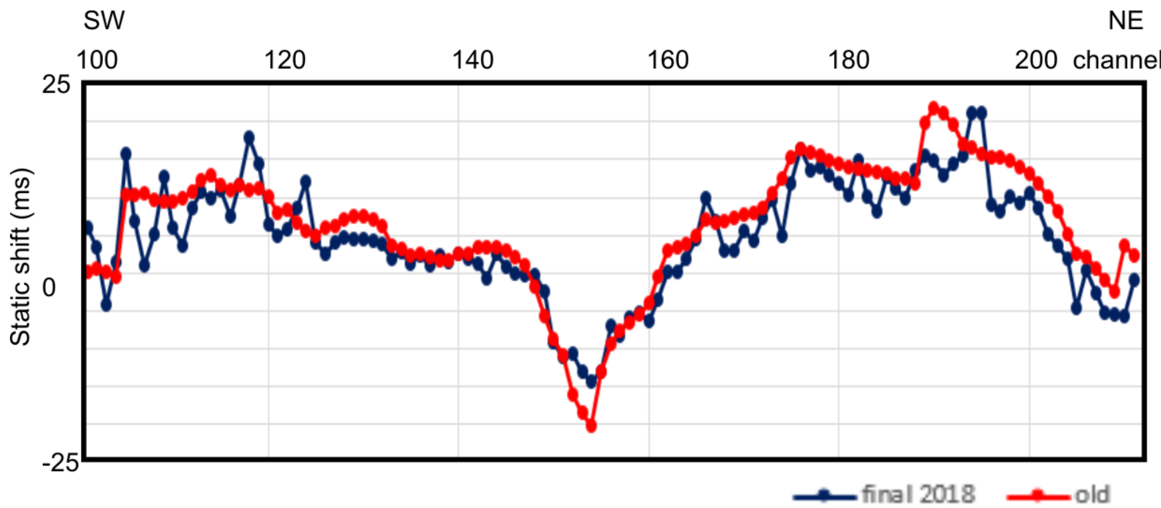

FIG. 11. Receiver statics applied to the data in Figure 8, derived from flattening receiver stacks compared to application of the receiver statics from the 2018 S-wave survey together with flattening the receiver stack.

CONCLUSIONS

The two S-wave seismic surveys acquired at the FRS in the summer of 2018 yielded useful and interesting data. Both surveys are about 1 km long but the first survey used receivers every 10 m in a 1-km fixed array while the second survey consisted of a 72-m towed streamer array with receivers every 1 m. The smoothed S-wave depth/velocity model derived from refraction statics analysis shows a 28.5 to 34.5 m thick near-surface S-wave low velocity layer with velocities ranging from 222 to 280 m/s. S-wave bedrock velocities range between 1045 and 1110 m/s. The depths to bedrock compare well with the actual bedrock depth of 29.5 m at the injection well location. The stacked streamer array line shows bedrock, and the depth-converted imaged bedrock compares very well with the true bedrock depth of 29.5 m at the injection well.

Application of the receiver statics derived from the fixed array survey to the PS data acquired in 2017 improved the imaging of the Basal Belly River reflector on stacked sections.

ACKNOWLEDGEMENTS

We thank CaMI.FRS JIP, CREWES sponsors for their financial support. This research was also in part supported by the Canada First Research Excellence Fund. We also gratefully acknowledge support from NSERC (Natural Science and Engineering Research Council of Canada) through the grant CRDPJ 461179-13. We appreciate the collaboration with Echo Seismic Ltd. and the generous contribution by Halliburton/Landmark for SeisSpace seismic data processing software.

REFERENCES

Margrave, G. F. and M. P. Lamoureux, 2002, Gabor deconvolution: CSEG Annual Convention Expanded Abstracts.